# An early signaling GARP transcription factor regulates the entry point for differentiation in *Giardia*

Han-Wei Shih, Germain C.M. Alas, Daria S. Rydell, Bailin Zhang, Greyson A. Hamilton, Benjamin Kerr, Alexander R. Paredez

Department of Biology, University of Washington, Seattle, Washington 98195

## Abstract

Transcriptional regulation of differentiation is critical for parasitic pathogens to adapt to environmental changes and regulate transmission. How early signaling transcription factors (TFs) activate signal transduction to initiate encystation remains an open question in *Giardia lamblia*. Here, we screened putative early signaling TFs with both a newly developed CasRX-mediated knockdown system and an established CRISPRi system to identify early signaling TFs that regulate encystation. We identified an early response TF, GARP4 that regulates Cyst Wall Protein (CWP) levels during encystation. Depletion of GARP4 increases cyst production. Interestingly, cyst viability and CWP1 trafficking are not altered in GARP4 knockdowns, suggesting GARP4 regulates the restriction point controlling the portion of cells that terminally differentiate into cysts. Consistent with previous studies, we find that stimulation of encystation shifts the distribution of cells to the G2/M phase and these cells exhibits higher levels of CWP1. Key to this increase of CWP1 in G2/M cells is activation of MYB2, a TF previously linked to the early phase of encystation in *Giardia*. Remarkably, activated GARP4 only exhibits in G1/S cells, suggesting it has a role in preventing encystation until G2/M. Furthermore, we demonstrate that depletion of GARP4 activates MYB2 and upregulates encystation while overexpression of GARP4 represses MYB2 and downregulates encystation. Our findings provide the first molecular mechanism underlying the restriction point regulating differentiation during early signaling of encystation in *Giardia lamblia*, which is a critical factor for optimizing parasite transmission.

## Introduction

To cope with environmental change, protozoa from all eukaryotic supergroups differentiate to dormant walled cysts, a process which is commonly called encystation[1]. For parasitic protozoa, deposition of a cyst wall is essential for antibiotic-resistance[2] and escape from the immune response[1]. Most importantly, water-resistant cysts allow parasitic protozoa to persist in fresh water and successfully transmit infection to susceptible hosts.

*Giardia* is a major cause of protozoan-based diarrhea and its encystation pathway plays an important role in pathogen virulence. *Giardia* infection often occurs through consuming

infectious cysts from contaminated water[3] or interpersonal contact[4]. Following passage of cysts through the acidic environment of stomach, they excyst in the duodenum and rapidly colonize the small intestine[5]. In the small intestine, cell density, lipid starvation and alkaline pH trigger a portion of trophozoites to initiate encystation[6-9]. During the early phase of *Giardia* encystation, major morphological changes occur that include cytoskeleton rearrangement, biogenesis of the Golgi-like ESVs, and cell cycle arrest[6,7,10].

Cell cycle arrest appears to be a common theme in encystation. Studies in *Giardia lamblia* [11], *Acanthamoeba* [12], and *Entamoeba invadens* [13] have all shown that encystation stimulus causes the accumulation of G2/M cells in the early stage of encystation. In *Acanthamoeba*, encystation frequency correlates with the proportion of cells arrested at G2[12], suggesting that differentiation is initiated from G2/M cells. These observations led to a hypothesis that a restriction point in *Giardia*'s cell cycle also limits encystation to cells in G2/M[11,14]. However, the molecular mechanism underlying this restriction point regulating entry into the encystation program is totally unknown.

Pioneer transcription factors (TFs), which are capable of binding condensed chromatin, possess the incredible ability to reprogram cell differentiation[15]. Several studied TFs in Giardia, such as GARP1[16], E2F1[17], WRKY[18], PAX2[19,20], ARID1[21] have been shown to be upregulated at 24 h post induction of encystation. A recent study has shown that a MYB TF is a master regulator of differentiation in *Toxoplasma* [22]. MYB TFs also modulate encystation in *Giardia*[23] and *Entamoeba*[24]. Proteomic and RNA sequencing studies agree that *Giardia*'s MYB2 TF is a key regulator of encystation[25-27]. While these observations hint that MYB2 may prompt the initiation of encystation, the upstream regulators of MYB2 are still poorly understood. Here, we screened *Giardia* transcription factors that were reported to be upregulated within 1.5-4 h of inducing encystation based on published RNAseq data[27]. A functional role in encystation was tested using an established dead Cas9 based CRISRPi system and a newly generated CasRX knockdown system that targets RNA for degradation. We identified GARP4 as an upstream regulator of MYB2 and determined that it has a key role in regulating entry into the encystation program.

## Results

### Characteristics of transcription factors during early encystation in *Giardia*

Given that CWP1-3 are important encystation indicators in *Giardia*[6,7,25,28,29], we first investigated CWP1-3 protein levels during the initiation of encystation using NanoLuc based expression reporters [30,31]. After exposure to encystation medium, CWP1-3 protein levels began to increase after 1.5h and rose exponentially by 4h (Fig 1a). To date, several TFs have been identified with roles in regulating CWP1-2, these include MYB2 [23], E2F1 [17], PAX1,2 [19,20], ARID1[21] and WRKY [18]. Whether these TFs have a role in initiating entry into the encystation pathway has not been established. The increase of CWPs is likely to be signaled through early response TFs,

which trigger the activation or repression of encystation specific genes. A previous transcriptomics study identified 11 TF candidates that are upregulated within 4 h of encystation [27]. We sought to test whether these TFs function as upstream regulators of encystation. Due to low confidence that some of the identified proteins weref in fact transcription regulators, we endogenously tagged the C-terminus of these 11 proteins with mNeonGreen (mNG) to verify nuclear localization, using MYB2 as a positive control. MYB2 expression has been detected 7 h post induction of encystation in proteomic[25] and RNA sequencing studies[27] and its function in encystation has been established. We were able to detect nuclear localization of MYB2 at 4 h but not at 0 and 1.5 h (Fig 1b). In contrast, we observed six TFs, including MYB1, GARP4, PAX1, ARID2, E2F1 with nuclear localization at 0 h but with noticeable increases in their levels after 1.5 h of encystation stimulus (Fig 1c; Extended data 1).

We then decided to investigate the expression level of these TFs. GARP4 and MYB1 rose nearly four folds after 1.5 h of inducing encystation, with GARP4 having the highest level of induction (Fig 1d). The expressions of PAX1, ARID2 and E2F1 only modestly increased by 4h (Extended data 2). That MYB1 and GARP4 are upregulated before MYB2 hints that these transcription factors may be early regulators of encystation that are upstream of MYB2 and CWP1.

**Depletion of MYB2, MYB1, and GARP4 alters the encystation response**

We next screened for encystation-specific TFs that are required for CWP1 synthesis, focusing on genes that were upregulated within 1.5 h of encystation. To screen for encystation specific TFs, we used an established dCas9 based CRISPRi system [28] and generated a complementary Cas13 knockdown system. Cas13 enzymes are RNA-targeting CRISPR enzymes which have been shown to have high efficiency and specificity in human cells[32]. We first tested the ability to express three Cas13 enzymes (Extended data 3a), including PsCas13b[33], CasRX[32] and EsCas13d[32]. CasRX was the only Cas13 enzyme with good expression in *Giardia* (Extended data 3b). Starting with the existing CRISPRi vector, we replaced dCas9 and the gRNA scaffold sequence (SCF) with CasRX and the CasRX-specific direct repeat (DR) (Extended data 3c), to establish a functional CasRX knockdown system. To determine if one of these knockdown systems might be better tolerated than the other, we examined the proportion of cells that expressed dCas9 or CasRX and found no appreciable difference (Extended data 3d,e). Moreover, the growth rate was essentially identical for dCas9 and CasRX expressing cell lines (Extended data 3f). To compare efficacy of knockdown, we designed CasRX- and CRISPRi-specific guide RNAs to deplete NanoLuc and CWP1. For these two genes CasRX outperformed CRISPRi reaching up to 80% reduction for CWP1 (Extended data 4). However, screening of gRNAs against the set of six TFs of interest revealed that efficacy varies by target gene and neither system is consistently better than the other.

As previous studies have suggested a critical role for MYB2 in *Giardia* encystation[23,34], we first investigated the phenotype of a CRISPRi-mediated MYB2 knockdown mutant (Fig 2a). Depletion

of MYB2 reduced the CWP1 and CWP2 level at 4h of encystation (Fig 2b,c, Extended data 5a) and totally abolished the maturation of cysts (Fig 2d; Extended data 6), suggesting MYB2 is essential for encystation. Notably, our data is consistent with a MYB2 antisense silencing mutant which reduces CWP1 expression[23]. Knockdown of MYB1 resulted in lower CWP1 and CWP2 levels (Fig 2e; Extended data 5a) and fewer encysting cell (Fig 2f,g); however after 48h the percentage of viable mature cysts (Fig 2h; Extended data 6c,d) was similar to the control. This suggests that MYB1 might be an upstream regulator of CWP1 but is not essential for cyst maturation. Interestingly, depletion of GARP4 results in a two-fold increase in CWP1 levels (Fig 2i) and an approximately 20% increase in CWP2 levels (Fig 2 j-k; Extended data 5a). Notably, GARP4 knockdown results in more mature cysts (Fig 2l) without changing cyst viability (Extended data 6a,b). We additionally determined that knockdown of E2F1 (Extended data 7a-c) and PAX1 (Extended data 7d-f) produced less CWP1 which agrees with published studies[17,20]. However, we unexpectedly found that, based on CWP1 expression, a higher proportion of the knockdown cell lines initiated the encystation pathway by 4h (Extended data 5c-d). Knockdown of ARID2 did not alter CWP1 levels (Extended data 7g-i) nor change the amount of encysting cells (Extended data 5d). In summary, these results show that GARP4 is a repressor of CWP1 and cyst development and that while MYB1 is an activator of CWP1, it is not essential for cyst maturation.

**Depletion of GARP4 upregulates encystation**

To further characterize the role of GARP4, we investigated whether depletion of GARP4 changes cell growth rate and cell viability. Knockdown of GARP4 does not alter proliferation or viability (Extended data 8a-b). In addition to the high bile Uppsala encystation method used above, *Giardia* can be encysted with additional methods that include the two-step method that removes bile and then provides bile levels moderately above the critical concentration for bile acid micelle formation to sequester cholesterol or cells can be starved for cholesterol with lipo-protein deficient media. Similar to the high bile Uppsala method, both two-step and lipo-protein deficient encystation media upregulated CWP1 more in the GARP4 mutant background (Extended data 8d), indicating GARP4 knockdown phenotype is not restricted to a specific encystation protocol. Considering that GARP4 has an important role in regulating encystation, we examined how its levels change over a fine time course at the induction of encystation. Remarkably, GARP4 levels shoot up at 30 minutes while MYB1 does not appreciably ramp up until after 60 minutes of encystation (Fig 3a). GARP4 mutants have consistently higher CWP1 levels during early encystation (Fig 3b). We analyzed individual cells to determine whether the increase of CWP1 in the GARP4 knockdown lines was due to increased numbers of cells entering the encystation program or resulted from increased levels of CWP1 per cell. We collected encysting cells from different time points of encystation and stained with a CWP1 antibody to quantify encysting cells. We then investigated various phenotypes of CWP1 trafficking in GARP4 mutants. The percentage of encysting cells is 1.5-2 fold higher in GARP4

mutants at 0, 1, 2, 4, 24 h treatments (Extended data 9; Fig 3c-d). Furthermore, we analyzed CWP1-positive vesicle size and volume to address if CWP1 trafficking in GARP4 mutant is altered. Our results show that neither vesicle size nor vesicle volume are changed (Fig 3e-f; Extended data 8c). Consistently, overexpression of GARP4 inhibits 50% of CWP1 expression (Extended data 8e,f). These findings suggest that the main role of GARP4 is to modulate the portion of cells that enter the differentiation pathway.

Given that cysts initiate new infections and a depletion of GARP4 leads to a higher rate of encystation, mutations that reduce GARP4 would appear to be selectively beneficial. However, the situation is more complicated because any trophozoite that forms a cyst will not produce descendant trophozoites that collectively could give rise to multiple cysts. Thus, if there is population of *Giardia* expanding inside an infected host, there is a tradeoff between current and future cyst production.

This tradeoff between short-term and long-term production can be captured by a simple dynamical model (see Methods). In brief, we assume that the population of trophozoites expands at a constant rate within the host and is shed at a constant rate from the host. In our model, trophozoites inside the host encyst at a constant rate (and cysts do not divide). We derive an expression giving the cumulative number of cysts as a function of the length of infection (as well as the initial number of cells and the rates of growth, shedding and encystation; see Methods). Using this expression, we determine the optimal encystation rate as a function of the other model parameters (Fig 3g). This optimal encystation rate decreases with an increasing period of infection, an increasing growth rate inside the host, and a decreasing rate of loss due to shedding. All else being equal, factors that make infections longer, more productive, or less prone to shedding are predicted to favor a longer term investment in cyst production via a *smaller* encystation rate.

One of the principal results from this model can be tested experimentally. Specifically, under a serial propagation scheme (see Methods), we predict that the GARP4 knockdown lines will exhibit higher cyst production in early transfers, but lower cyst production in late transfers, relative to wild type. This is indeed the pattern that we see (Fig 3h). Furthermore, we see that the long-term cost of a higher encystation rate is a relative decrease in the trophozoite population (Fig 3i).

## GARP4 functions in the G1/S phase of the cell cycle

Encystation-induced G2 arrest has been demonstrated in *Giardia* [35,36]. Indeed, our data is consistent with previous studies that 1.5 h of encystation is sufficient to cause accumulation of G2/M cells with a corresponding reduction of cells in G1/S (Fig 4a-b). To investigate whether cells in G2/M have higher CWP1, mNG-tagged CWP1 cell lines were exposed to encystation stimuli and then DNA content was measured by DRAQ5 fluorescence. We found that cells with higher DNA content had higher CWP1 levels (Extended data 10a). Similarly, G2/M cells have

higher MYB2 levels (Extended data 10b), suggesting higher expression of CWP1 was due to higher level of MYB2. A prior study in *Giardia* has suggested the presence of a restriction point for entering encystation that functions to prevent cells in G1/S from initiating encystation but permits cells in G2/M to differentiate. It seemed possible that GARP4 might inhibit G1 cells from initiating encystation. We examined the relationship between GARP4-mNG and the cell cycle at 0 and 1.5 h of encystation. We found that GARP4-mNG fluorescence intensity was 1.5 fold increased in G1/S cells after exposure to encystation stimuli but slightly decreased in cells at G2/M, suggesting lower GARP4 levels permit G2/M cells to enter encystation. Because MYB2 and CWP1 levels are lower in G1 cells, we questioned if GARP4 might be an upstream repressor of MYB2. We transfected the GARP4 CRISPRi guide RNA into MYB2-NanoLuc cell line. We found that MYB2 levels rose by 1.2 fold in the GARP4 knockdown cell line, which is consistent with MYB2 ultimately regulating CWP1 levels (Fig 4d). In contrast, overexpression of GARP4 inhibited MYB2 expression by 50% and resulted in reduced CWP1 levels (Fig 4e-f). These findings suggest MYB2 is downstream of GARP4.

Since E2F1 and PAX1 have been shown to regulate CWP1-3 and MYB2, we sought to determine whether GARP4 modulates MYB2 through either E2F1 or PAX1. Interestingly, knockdowns of GARP4 does not alter E2F1 or PAX1 levels (Extended data 10c-d), suggesting E2F1 and PAX1 are not part of GARP4-MYB2-CWP1 pathway. Thus, MYB2 is a downstream of GARP4 but an upstream regulator of CWP1. In this model, MYB2 is repressed in cells at G1/S by GARP4, then during G2/M GARP4 levels drop and MYB2 expression is triggered to induce encystation.

## Discussion

In summary, we utilized CRISPRi and our newly developed CasRX-mediated knockdown tool to identify transcription factors that regulate entry into the encystation pathway. We identified GARP4, a previously unstudied TF, as a key regulator of *Giardia*'s restriction point regulating differentiation. GARP TFs are commonly considered to be plant-specific, but are also found in protists. Some plant GARP TFs are pioneering TFs for reproductive organ determination[37]. In this study, we found that GARP4 functions to prevent cells in G1/S from entering the encystation program. Our results provide the molecular mechanism for the restriction point that prevents entry into encystation until cells arrest in G2/M. We found that GARP4 depletion upregulates the formation of healthy cysts and therefore GARP4 is not required for cyst formation. Instead, GARP4 likely regulates the balance of parasite load, which selective pressure is expected to have optimized for maximal transmission. When exposed to encystation stimulus, GARP4 expression is triggered in the G1/S population to repress CWP1 level through inhibiting MYB2. In contrast, GARP4 levels in the G2/M population is slightly decreased, thus allowing the activation of MYB2 to enhance CWP1 production. Our model explains why the frequency of G2/M cells have higher expression of CWP1.

How cells sense encystation stimulus but then induce different responses based on cell cycle status remains unknown in *Giardia*. The idea that histone deacetylase may be involved in encystation regulation is quite attractive given the function as a metabolic sensor for rapid environment sensing. Only Sirutin 2.1 (GL50803_10708) is highly expressed at early phase of encystation[27]. Interestingly, Sirtuin inhibitor Nicotinamide has been shown to cause G2 arrest of cell cycle[38]. However, our data indicates that mNG-tagged Sirtuin 2.1 only localizes to cytosol at 0 and 1.5 h of encystation (Extended data 10 e,f) which is consistent with other studies[39], suggesting Sirtuin 2.1 is not involved in regulating early encystation. It will be of particular interest to test whether second messengers have a role in coordinating early encystation, or act as a molecular switch to initiate differentiation into cysts.

## Methods

### Giardia growth and encystation media

*Giardia intestinalis* isolate WB clone C6 (ATCC catalog number 50803; American Type culture collection) were cultured in TYDK media at pH 7.1 supplemented with 10% adult bovine serum and 0.125 mg/ml bovine bile[40]. To induce encystation, cells were cultured 48 h in pH 6.8 pre-encystation media without bile then three encystation protocols were used: (1) Uppsala encystation protocol: TYDK media at pH 7.8 supplemented with 10% adult bovine serum and 5 mg/ml bovine bile[27]; (2) Two-step protocol: TYDK media at pH 7.8 supplemented with 10% adult bovine serum, 0.25 mg/ml porcine bile and 5 mM lactic acid[41]; (3) Lipoprotein-deficient protocol: TYDK media at pH 7.8 supplemented with lipoprotein-deficient serum[42].

### Plasmid construction

### mNeonGreen and NanoLuc fusions

Coding sequences were PCR-amplified from *Giardia lamblia* genomic DNA. Primers sequences are indicated in supplemental excel file. The mNeonGreen and NanoLuc vectors were digested with the indicated restriction enzymes and a PCR amplicon was ligated using Gibson assembly[43]. The resulting constructs were linearized with the restriction enzyme indicated in supplemental excel file before electroporation for integration into the endogenous locus[44]. Neomycin and puromycin were used for selection.

### CasRX expression cassette design

EsCas13d (Catalog #108303), CasRX (Cat #109049), and PspCas13b (Cat#103862) were obtained from Addgene. Cas 13 fragments were PCR amplified, digested with restriction enzymes and inserted into pPAC-3HA expression cassettes under GDH promoter[45]. The Cas13-3HA expression vectors were linearized with SwaI and electroporated into *Giardia lamblia*. To generate CasRX expression system, CRISPRi expression vector (dCas9g1pac) was used as a backbone.

## Design of guide RNA

Guide RNA for the CRISPRi system utilized the Dawson Lab protocol [28], NGG PAM sequence and G. Lamblia ATCC 50803 genome were selected for CRISPRi guide RNA design with Benchling. Cas13 guide RNA designs were based on the Sanjana Lab Cas13 guide tool (https://cas13design.nygenome.org/)[46].

## In vitro bioluminescence assays

*Giardia* cells were iced for 15 min and centrifuged at 700 x g for 7 min at 4°C. Cells were resuspended in cold 1X HBS (HEPES-buffered saline) and serial dilutions were made using a MOXI Z mini Automated Cell Counter Kit (Orflo, Kenchum, ID). To measure NanoLuc luminescence, 20,000 cells were loaded into white polystyrene, flat bottom 96-well plates (Corning Incorporated, Kennebunk, ME) then mixed with 10 µl of NanoGlo luciferase assay reagent (Promega). Relative luminescence units (RLU) were detected on a pre-warmed 37°C EnVision plate reader (Perkin Elmer, Waltham, MA) for 30 min to reach the maximum value. Experiments are from three independent bioreplicates. To measure CBG99 luminescence, 20,000 cells were loaded into white polystyrene, flat bottom 96-well plates then mixed with 50 µl of 10 mg/mL D-luciferin. Relative luminescence units (RLU) were detected as above.

## Protein blotting

*Giardia* parasites were iced for 30 min then centrifuged at 700 x g for 7 min and washed twice in 1X HBS supplemented with HALT protease inhibitor (Pierce) and phenylmethylsulfonyl fluoride (PMSF). The cells were resuspended in 300 µl of lysis buffer contains 50 mM Tris-HCl pH 7.5, 150 mM NaCl, 7.5% glycerol, 0.25 mM $CaCl_2$, 0.25 mM ATP, 0.5 mM Dithiotheitol, 0.5 mM PMSF (Phenylmethylsulfonyl flroride), 0.1% Trition X-100 and Halt protease inhibitors (Pierce). The sample was pelleted at 700 x g for 7 min, the supernatant was mixed with 2X sample buffer (Bio-Rad) and boiled at 98°C for 5 min. Protein samples were separated using sodium dodecyl sulfate (SDS) polyacriamide gel electrophoresis. Protein transfer was performed using an Immobilon-FL membrane (Milipore). To detect tubulin, a mouse monoclonal anti-acetylated tubulin clone 6-11B-1 antibody (IgG2b; product T 6793; Sigma-Aldrich) were used at 1:2,500 and secondary anti-mouse isotype-specific antibody conjugated with Alexa 488 (anti-IgG2b) were used at 1:2,500. To detect CWP1, Alexa 647-conjugated anti-CWP1 antibody (Waterborne, New Orleans, LA) was used at 1:2,000. Multiplex immunoblots were imaged using a Chemidoc MP system (Bio-Rad).

## Immunofluorescence

*Gairdia* parasites were iced for 30 min and pelleted at 700 x g for 7 min. The pellet was fixed in PME buffer (100 mM Piperazine-N,N'-bis (ethanesulfonic acid) (PIPES) pH 7.0, 5 mM EGTA, 10 mM $MgSO_4$ supplemented with 1% paraformaldehyde (PFA) (Electron Microscopy Sciences, Hatfield, PA), 100 µM 3-maleimidobenzoic acid N-hydroxysuccinimide ester (Sigma-Aldrich), 100 µM ethylene glycol bis (succinimidyl succinate) (Pierce), and 0.025% Triton X-100 for 30 min

at 37°C. Fixed cells were attached on polylysine coated coverslips. Cells were washed once in PME and permeabilized with 0.1% Triton X-100 in PME for 10 min. After two quick washes with PME, blocking was performed in PME supplemented with 1% bovine serum albumin, 0.1% $NaN_3$, 100 mM lysine, 0.5% cold water fish skin gelatin (Sigma-Aldrich). Next, 1:200 diluted Alexa 647-conjugated anti-CWP1 antibody (Waterborne, New Orleans, LA) was added to incubate for 1 h. Cells were washed three times in PME plus 0.05% Triton X-100. Coverslips were mounted with ProLong Gold antifade plus 4',6-diamidino-2-phenylinodole (DAPI; Molecular Probes). Images were acquired on a DeltaVision Elite microscope using a 60X, 1.4-numerical aperture objective with a PCO Edge sCMOS camera, and images were deconvolved using SoftWorx (API, Issaquah, WA).

**Imaging and image analysis**

Analyses of CWP1-stained vesicle size and number were performed with Imaris software (Bitplane, version 8.1). ImageJ was used to process all images and figures were assembled using Adobe Illustrator.

**Cyst count and cyst viability staining**

To collect water-resistant *Giardia* cysts, confluent *Giardia* trophozoites were incubated in encystation media supplemented with 10 g/L ovine bovine bile and calcium lactate. To count cyst, 20 µl of 48 h encysted cells were counted using a hemocytometer. To determine cyst viability, 48 h encysted *Giardia* cells were centrifuged at 700 x g for 7 min and the pellets were washed 10 times in deionized water, then stored in distill water overnight at 4°C. Next day, fluorescein diacetate (FDA) and propidium iodide (PI) were used to stain live and dead cysts and collected images using a DeltaVision Elite microscope using a 40X, 1.4-numerical apeture objective with a PCO Edge sCMOS camera, and images were deconvolved using SoftWorx (API, Issaquah, WA).

**Flow cytometry assay**

Flow cytometry analyses was performed after fixation with 0.25% PFA at 4°C for 15 min. 1 µM DRAQ5 (Thermo Scientific Cat# 62251) was used to stain DNA. 10,000 cells per sample were analyzed using a FACS Canto II Flow Cytometer at the Pathology Flow Cytometry Core Facility (Department of Pathology, University of Washington). Data were analyzed using FlowJo.

**Mathematical modeling**

We let the number of trophozoites inside an infected host be $T_t$ and the number of cysts produced during infection be $C_t$. Assuming constant rates for growth, shedding and encystation, the following differential equations describe the change in cell numbers

$$\dot{T}_t = (\gamma - \lambda - \varepsilon)T_t, \qquad [1.1]$$

$$\dot{C}_t = \varepsilon T_t, \qquad [1.2]$$

with $\gamma$ as the rate of population growth of the trophozoites inside the host, $\lambda$ as rate at which cells are lost from the host via shedding, and $\varepsilon$ as the rate of encystation inside the host, and the dot over the dynamical variables indicating differentiation with respect to time. We note that cysts that leave the host are counted in the total number of produced cysts, but trophozoites that leave the host can no longer contribute to further growth or cyst production. Equations [1] have the following solution:

$$T_t = T_0 e^{(\gamma-\lambda-\varepsilon)t}, \qquad [2.1]$$

$$C_t = C_0 + T_0 \frac{\varepsilon\left(e^{(\gamma-\lambda-\varepsilon)t} - 1\right)}{\gamma - \delta - \varepsilon}. \qquad [2.2]$$

In this model, the trophozoite population expands exponentially (if $\gamma - \lambda > \varepsilon$). We can use equation [2.2] to determine numerically the optimal encystation rate ($\varepsilon^*$) to maximize the total number of cysts produced as a function of the length of the infection period ($t$) and other model parameters ($C_0$, $T_0$, $\gamma$, and $\lambda$). For simplicity, we assume that an infection is initiated by a single trophozoite ($C_0 = 0$ and $T_0 = 1$). For our baseline growth rate, we used a best-fit estimate from Giardia in encystation medium ($\gamma = 0.363$) and for the high growth rate, we used a best-fit estimate from Giardia in TYDK medium ($\gamma = 0.762$). For the shedding rates, we used $\lambda = 0.1$ and $\lambda = 0.25$ as the baseline and high values, but the basic patterns shown in Fig. 3g also held for other values of shedding.

**Acknowledgements**

We thank members of the Paredez laboratory and our colleagues at UW Biology for discussions and comments on the manuscripts, and a big help from the flow cytometry facility at UW Pathology. We thank Photini Sinnis, Kirk Deitsch, Patricia Johnson for inviting us to participate in the 40th-Biology of Parasitism (BoP) course and all of the help from BoP students to initiate this project. We thank Dr. Scott Dawson for gifting us the CRISPRi plasmid. Research was funded by University of Washington Bridge funds and NIAD 1R21AI159035 to ARP.

1 Schaap, P. & Schilde, C. Encystation: the most prevalent and underinvestigated differentiation pathway of eukaryotes. *Microbiology (Reading, England)* **164**, 727-739, doi:10.1099/mic.0.000653 (2018).

2 Kumar, R. & Lloyd, D. Recent advances in the treatment of Acanthamoeba keratitis. *Clinical infectious diseases : an official publication of the Infectious Diseases Society of America* **35**, 434-441, doi:10.1086/341487 (2002).

3 Fakhri, Y. *et al.* The risk factors for intestinal Giardia spp infection: Global systematic review and meta-analysis and meta-regression. *Acta tropica*, 105968, doi:10.1016/j.actatropica.2021.105968 (2021).

4 Waldram, A., Vivancos, R., Hartley, C. & Lamden, K. Prevalence of Giardia infection in households of Giardia cases and risk factors for household transmission. *BMC infectious diseases* **17**, 486, doi:10.1186/s12879-017-2586-3 (2017).

5 Wright, S. G. Protozoan infections of the gastrointestinal tract. *Infectious disease clinics of North America* **26**, 323-339, doi:10.1016/j.idc.2012.03.009 (2012).

6 Argüello-Garciá, R., Bazán-Tejeda, M. L. & Ortega-Pierres, G. Encystation commitment in Giardia duodenalis: a long and winding road. *Parasite (Paris, France)* **16**, 247-258, doi:10.1051/parasite/2009164247 (2009).

7 Lauwaet, T., Davids, B. J., Reiner, D. S. & Gillin, F. D. Encystation of Giardia lamblia: a model for other parasites. *Current opinion in microbiology* **10**, 554-559, doi:10.1016/j.mib.2007.09.011 (2007).

8 Luján, H. D., Mowatt, M. R., Byrd, L. G. & Nash, T. E. Cholesterol starvation induces differentiation of the intestinal parasite Giardia lamblia. *Proceedings of the National Academy of Sciences* **93**, 7628-7633, doi:10.1073/pnas.93.15.7628 (1996).

9 Barash, N. R. *et al.* Giardia Colonizes and Encysts in High-Density Foci in the Murine Small Intestine. *mSphere* **2**, doi:10.1128/mSphere.00343-16 (2017).

10 Faso, C. & Hehl, A. B. Membrane trafficking and organelle biogenesis in Giardia lamblia: use it or lose it. *International journal for parasitology* **41**, 471-480, doi:10.1016/j.ijpara.2010.12.014 (2011).

11 Bernander, R., Palm, J. E. & Svärd, S. G. Genome ploidy in different stages of the Giardia lamblia life cycle. *Cellular microbiology* **3**, 55-62, doi:10.1046/j.1462-5822.2001.00094.x (2001).

12 Byers, T. J., Kim, B. G., King, L. E. & Hugo, E. R. Molecular aspects of the cell cycle and encystment of Acanthamoeba. *Reviews of infectious diseases* **13 Suppl 5**, S373-384, doi:10.1093/clind/13.supplement_5.s373 (1991).

13 Eichinger, D. Encystation of entamoeba parasites. *BioEssays : news and reviews in molecular, cellular and developmental biology* **19**, 633-639, doi:10.1002/bies.950190714 (1997).

14 Svärd, S. G., Hagblom, P. & Palm, J. E. D. Giardia lamblia — a model organism for eukaryotic cell differentiation. *FEMS Microbiology Letters* **218**, 3-7, doi:10.1111/j.1574-6968.2003.tb11490.x (2003).

15 Larson, E. D., Marsh, A. J. & Harrison, M. M. Pioneering the developmental frontier. *Molecular cell* **81**, 1640-1650, doi:10.1016/j.molcel.2021.02.020 (2021).

16 Sun, C. H., Su, L. H. & Gillin, F. D. Novel plant-GARP-like transcription factors in Giardia lamblia. *Molecular and biochemical parasitology* **146**, 45-57, doi:10.1016/j.molbiopara.2005.10.017 (2006).

17 Su, L.-H. *et al.* A Novel E2F-like Protein Involved in Transcriptional Activation of Cyst Wall Protein Genes in Giardia lamblia*. *Journal of Biological Chemistry* **286**, 34101-34120, doi:https://doi.org/10.1074/jbc.M111.280206 (2011).

18 Pan, Y. J., Cho, C. C., Kao, Y. Y. & Sun, C. H. A novel WRKY-like protein involved in transcriptional activation of cyst wall protein genes in Giardia lamblia. *J Biol Chem* **284**, 17975-17988, doi:10.1074/jbc.M109.012047 (2009).

19 Chuang, S.-F., Su, L.-H., Cho, C.-C., Pan, Y.-J. & Sun, C.-H. Functional Redundancy of Two Pax-Like Proteins in Transcriptional Activation of Cyst Wall Protein Genes in Giardia lamblia. *PLOS ONE* **7**, e30614, doi:10.1371/journal.pone.0030614 (2012).

20 Wang, Y.-T. *et al.* A novel pax-like protein involved in transcriptional activation of cyst wall protein genes in Giardia lamblia. *J Biol Chem* **285**, 32213-32226, doi:10.1074/jbc.M110.156620 (2010).

21 Wang, C. H., Su, L. H. & Sun, C. H. A novel ARID/Bright-like protein involved in transcriptional activation of cyst wall protein 1 gene in Giardia lamblia. *J Biol Chem* **282**, 8905-8914, doi:10.1074/jbc.M611170200 (2007).

22 Waldman, B. S. *et al.* Identification of a Master Regulator of Differentiation in Toxoplasma. *Cell* **180**, 359-372.e316, doi:10.1016/j.cell.2019.12.013 (2020).

23 Sun, C.-H., Palm, D., McArthur, A. G., Svärd, S. G. & Gillin, F. D. A novel Myb-related protein involved in transcriptional activation of encystation genes in Giardia lamblia. *Molecular Microbiology* **46**, 971-984, doi:https://doi.org/10.1046/j.1365-2958.2002.03233.x (2002).

24 Ehrenkaufer, G. M., Hackney, J. A. & Singh, U. A developmentally regulated Myb domain protein regulates expression of a subset of stage-specific genes in Entamoeba histolytica. *Cellular microbiology* **11**, 898-910, doi:10.1111/j.1462-5822.2009.01300.x (2009).

25 Faso, C., Bischof, S. & Hehl, A. B. The proteome landscape of Giardia lamblia encystation. *PLoS One* **8**, e83207, doi:10.1371/journal.pone.0083207 (2013).

26 Pham, J. K. *et al.* Transcriptomic Profiling of High-Density Giardia Foci Encysting in the Murine Proximal Intestine. *Frontiers in cellular and infection microbiology* **7**, doi:10.3389/fcimb.2017.00227 (2017).

27 Einarsson, E. *et al.* Coordinated Changes in Gene Expression Throughout Encystation of Giardia intestinalis. *PLOS Neglected Tropical Diseases* **10**, e0004571, doi:10.1371/journal.pntd.0004571 (2016).

28 McInally, S. G. *et al.* Robust and stable transcriptional repression in Giardia using CRISPRi. *Molecular biology of the cell* **30**, 119-130, doi:10.1091/mbc.E18-09-0605 (2019).

29 Pham, J. K. *et al.* Transcriptomic Profiling of High-Density Giardia Foci Encysting in the Murine Proximal Intestine. *Frontiers in cellular and infection microbiology* **7**, 227, doi:10.3389/fcimb.2017.00227 (2017).

30 Masser, A. E., Kandasamy, G., Kaimal, J. M. & Andréasson, C. Luciferase NanoLuc as a reporter for gene expression and protein levels in Saccharomyces cerevisiae. *Yeast (Chichester, England)* **33**, 191-200, doi:10.1002/yea.3155 (2016).

31 England, C. G., Ehlerding, E. B. & Cai, W. NanoLuc: A Small Luciferase Is Brightening Up the Field of Bioluminescence. *Bioconjugate chemistry* **27**, 1175-1187, doi:10.1021/acs.bioconjchem.6b00112 (2016).

32 Konermann, S. *et al.* Transcriptome Engineering with RNA-Targeting Type VI-D CRISPR Effectors. *Cell* **173**, 665-676.e614, doi:10.1016/j.cell.2018.02.033 (2018).

33 Cox, D. B. T. *et al.* RNA editing with CRISPR-Cas13. *Science (New York, N.Y.)* **358**, 1019-1027, doi:10.1126/science.aaq0180 (2017).

34 Huang, Y.-C. *et al.* Regulation of Cyst Wall Protein Promoters by Myb2 in Giardia lamblia*. *Journal of Biological Chemistry* **283**, 31021-31029, doi:https://doi.org/10.1074/jbc.M805023200 (2008).

35 Reiner, D. S. *et al.* Synchronisation of Giardia lamblia: identification of cell cycle stage-specific genes and a differentiation restriction point. *International journal for parasitology* **38**, 935-944, doi:10.1016/j.ijpara.2007.12.005 (2008).

36 Dawson, S. C., Nohýnková, E. & Cipriano, M. in *Giardia: A Model Organism* (eds Hugo D. Luján & Staffan Svärd) 161-183 (Springer Vienna, 2011).

37 Safi, A. *et al.* The world according to GARP transcription factors. *Current opinion in plant biology* **39**, 159-167, doi:10.1016/j.pbi.2017.07.006 (2017).

38 Lagunas-Rangel, F. A., Bazán-Tejeda, M. L., García-Villa, E. & Bermúdez-Cruz, R. M. Nicotinamide induces G2 cell cycle arrest in Giardia duodenalis trophozoites and promotes changes in sirtuins transcriptional expression. *Experimental Parasitology* **209**, 107822, doi:https://doi.org/10.1016/j.exppara.2019.107822 (2020).

39 Herrera T, E. A., Contreras, L. E., Suárez, A. G., Diaz, G. J. & Ramírez, M. H. GlSir2.1 of Giardia lamblia is a NAD+-dependent cytoplasmic deacetylase. *Heliyon* **5**, e01520, doi:https://doi.org/10.1016/j.heliyon.2019.e01520 (2019).

40 Keister, D. B. Axenic culture of Giardia lamblia in TYI-S-33 medium supplemented with bile. *Transactions of the Royal Society of Tropical Medicine and Hygiene* **77**, 487-488, doi:10.1016/0035-9203(83)90120-7 (1983).

41 Gillin, F. D., Boucher, S. E., Rossi, S. S. & Reiner, D. S. Giardia lamblia: the roles of bile, lactic acid, and pH in the completion of the life cycle in vitro. *Exp Parasitol* **69**, 164-174, doi:10.1016/0014-4894(89)90185-9 (1989).

42 Luján, H. D., Mowatt, M. R., Byrd, L. G. & Nash, T. E. Cholesterol starvation induces differentiation of the intestinal parasite Giardia lamblia. *Proceedings of the National Academy of Sciences of the United States of America* **93**, 7628-7633, doi:10.1073/pnas.93.15.7628 (1996).

43 Gibson, D. G. *et al.* Enzymatic assembly of DNA molecules up to several hundred kilobases. *Nature Methods* **6**, 343-345, doi:10.1038/nmeth.1318 (2009).

44 Gourguechon, S., Holt, L. J. & Cande, W. Z. The Giardia cell cycle progresses independently of the anaphase-promoting complex. *Journal of cell science* **126**, 2246-2255, doi:10.1242/jcs.121632 (2013).

45 Gourguechon, S. & Cande, W. Z. Rapid tagging and integration of genes in Giardia intestinalis. *Eukaryotic cell* **10**, 142-145, doi:10.1128/ec.00190-10 (2011).

46 Wessels, H. H. *et al.* Massively parallel Cas13 screens reveal principles for guide RNA design. *Nature biotechnology* **38**, 722-727, doi:10.1038/s41587-020-0456-9 (2020).

**Figure 1 | GARP4 and MYB1 are early signaling TFs. a**, Quantification of endogenously tagged CWP1-NLuc, CWP2-NLuc, and CWP3-NLuc after 0, 1.5, and 4 h exposure to encystation medium (Uppsala medium). Expression level from each time point has three biological replicates. Fold change is normalized to 0 h. **b**, Localizations of MYB2-mNG after 0, 1.5, and 4 h exposure to Uppsala medium. **c**, Localizations of PAX1-mNG, GARP4-mNG and MYB1-mNG after 0 and 1.5 h exposure to Uppsala medium. **d**, Relative expression of GARP4-NLuc, MYB1-NLuc, MYB2-NLuc, and GAPDH-NLuc after 0, 1.5, 4, 7h exposure to Uppsala medium. Expression level from each time point has three biological replicates. The fold change is normalized to 0 h. Bars, 10 µm.

**Figure 2 | Depletion of GARP4 increases CWP1 level and cyst number. a**, Quantification of CRISPRi-mediated knockdowns of MYB2 at 4h into encystation. The expression level is normalized by a dCas9 control. **b**, Immunoblot of CWP1 and tubulin from MYB2 knockdowns at 4h into encystation. **c**, Quantification of immunoblots of CWP1 and tubulin from MYB2 knockdowns. The expression level is normalized to tubulin. **d**, Quantification of cysts for MYB2 knockdown and control after 48 h of encystation. Cyst counts were performed by hemocytometer. **e**, Quantification of CRISPRi-mediated knockdown of MYB1 at 1.5h into encystation. **f**, Immunoblot of CWP1 and tubulin from MYB1 knockdown at 4h into encystation. **g**, Quantification of immunoblots of CWP1 and tubulin from MYB1 knockdowns at 4h into encystation. **h**, Quantification of cysts for MYB1 knockdown and control after 48 h of encystation. **i**, Quantification of CRISPRi-mediated knockdown of GARP4 at 1.5h into encystation. **j**, Immunoblot of CWP1 and tubulin from GARP4 knockdown at 4h into encystation. **k**, Quantification of immunoblots of CWP1 and tubulin from GARP4 knockdown. **l**, Quantification of cyst number of GARP4 knockdown after 48 h encystation. All quantification is from three independent biological replicates which included four technical replicates for cyst counts. Data are mean ± s.d. Student's t-test, *p<0.01, **p<0.001, ***p<0.0001, ****p<0.00001, ns= not significant.

**Figure 3| GARP4 regulates encystation rates. a**, Relative protein levels of MYB1-NLuc, MYB2-NLuc, and GARP4-NLuc after 0, 0.5, 1 and 2 h exposure to encystation medium (Uppsala medium). The expression level from each time point has three biological replicates. The fold change is normalized to 0 h. **b**, Relative expression of CWP1-NLuc in GARP4 knockdowns after 0, 0.5, 1,2,3 and 4 h exposure to encystation medium (Uppsala medium). The expression level from each time point has three biological replicates. The fold change is normalized to 0 h dCas9-Ctrl. **c**, CWP1 and DAPI staining at 24 h of encystation for dCas9-Ctrl, GARP4-gRNA247 and GARP4-gRNA362 cell lines. Bars, 100 µm. **d**, Quantification of encysting cells at 24 h post induction of encystation

for dCas9-Ctrl, GARP4-gRNA247 and GARP4-gRNA362 cell lines as determined by CWP1 expression. Data are mean ± s.d. from three independent experiments (total cells counted for dCas9-Ctrl n=1830, GARP4-g362 n=1747, GARP4-g247 n=1783) Student's t-test, *p<0.01. **e**, IMARIS-assisted analysis of vesicle number in 4 h encysting cells of dCas9-Ctrl, GARP4-gRNA247 and GARP4-gRNA362 cell lines. **f**, IMARIS-assisted analysis of vesicle volume of 4 h encysting cells of dCas9-Ctrl, GARP4-gRNA247 and GARP4-gRNA362 cell lines. n.s.= not significant. n=63 cells for dCas9-Ctrl. n= 93 for GARP4-g362. **g,** Using our dynamical model, we numerically determine the optimal encystation rate as a function of the period of infection for a baseline set of parameters (specifically, $\gamma = 0.363$ day$^{-1}$, $\lambda = 0.1$ day$^{-1}$, $T_0 = 1$ cell, and $C_0 = 0$ cells; see Methods). The result is the thick black curve. We then repeat the analysis but increase the rate of trophozoite growth ($\gamma = 0.762$ day$^{-1}$) or increase the rate of shedding ($\lambda = 0.25$ day$^{-1}$), which yields the blue and red curves, respectively. **h,** Quantification of cyst number in GARP4 knockdown from daily supplement of fresh encystation medium (removed detached cells and cysts). **i,** Quantification of trophozoite number in GARP4 knockdown from daily supplement of fresh encystation medium.

**Figure 4| GARP4 is part of the restriction point that prevents G1 cells from encysting. a**, Flow cytometry analysis of DRAQ5 and GARP4-mNG at 0 and 1.5 h of encystation. Red line is the separation point between G1/S and G2/M phases. **b**, Quantification of G1/S and G2/M cells from 0 and 1.5 h encystation. Data are mean ± s.d. (n=3, 10,000 cells per replicate) Student's t-test, **p<0.001. **c**, Quantification of GARP4-mNG fluorescence intensity for G1/S and G2/M cells at 0 and 1.5 h of encystation. Data are mean ± s.d. (n=3) Student's t-test, ****p<0.0001. **d**, Quantification of relative expressions of MYB2 from dCas9 control and GARP4-gRNA362 cell lines. ****p<0.00001. **e**, Fluorescent imaging of pTET::GARP4-mNG with and without tetracycline induction. Bars, 10 µm. **f,** Quantification of relative expressions of MYB2 after 4 h of encystation from tetracycline-induced GARP4-mNG overexpression cell lines. ****p<0.00001.

**Extended Data Figure 1| Localizations of encystation-induced genes.** Localizations of mNG-tagged E2F1 (GL50803_23756), GARP3 (GL50803_9154), PAX1 (GL50803_32686), CCAAT-binding subunit C (GL50803_14553), CCR4-NOT subunit 7 (GL50809_8209), CCAAT-binding subunit A (GL50803_7231) and CCR-NOT subunit 7 (GL50803_10606) after 0 and 1.5 h exposure to Uppsala encystation medium. Bars, 10 µm.

**Extended Data Figure 2| E2F1, PAX1 and ARID2 are induced at 4h.** Relative expression of E2F1-NLuc, PAX1-NLuc, ARID2-NLuc, and GAPDH-NLuc after 0, 1.5, 4, 7h exposure to Uppsala medium. The expression level from each time point has three biological replicates. The fold change is normalized by 0 h. E2F1, PAX, and ARID2 are significantly upregulated at 4 h.

**Extended Data Figure 3| *Giardia* CRISPRi and CasRX design. a-b**, Heterologous expression of 3HA tagged PsCas13b, CasRX, and EsCas13d in *Giardia*. pGDH= promoter of glyceraldehye 3-

phosphate dehydrogenease (GL50803_6877). HA=Hemagglutinin. **c**, Schematic of CRISPRi vector dCas9g1pac and CasRX vector design. pMDH= promoter of malate dehydrogenase, pac=puromycin resistance marker, 2340NLS=GL50803_2340 nuclear localization signal, SCF=gRNA scaffold sequence, DR=Direct repeat for CasRX, pU6=Giardia U6 promoter. **d**, Localizations of 3XHA tagged dCas9 and CasRX with DAPI staining in *Giardia*. **e,** Quantification of cells with detectable dCas9 and CasRX expression. ns=not significant. Data are mean ± s.d. from three independent experiments (dCas9 n=3278, CasRX n=3327 cells) Student's t-test. **f,** Growth curve of dCas9 and CasRX expressing cell lines. Blue=CasRX, Red=dCas9. Bars, 100 µm.

**Extended Data Figure 4| Screen of guide RNAs with CRISPRi and CasRX systems. a-h,** Relative quantification of protein levels using the indicated CRISPRi or CasRX gRNAs. Levels were normalized to non-specific gRNA controls. **a**, Quantification of CWP1 (GL50803_5638). **b,** Quantification of NanoLuc levels. **c,** Quantification of MYB1 levels (GL50803_5347). **d,** Quantification of ARID2 levels (GL50803_8102). **e,** Quantification of E2F1 levels (GL50803_23756). **f,** Quantification of PAX1 levels (GL50803_32686). **g,** Quantification of GARP4 levels (GL50803_33232). **h,** Quantification of MYB2 levels (GL50803_8722). All experiments are from three independent biological replicates. Data are mean ± s.d. (n=3) Student's t-test, *p<0.01, **p<0.001, ***p<0.0001, ****p<0.00001, ns= not significant.

**Extended Data Figure 5| Proportion of cells encysting after inducting encystation for 4 h in knockdowns of E2F1, PAX1 and ARID2. a**, Relative CWP2 levels in knockdowns of MYB1, GARP4 and MYB2 4 h post induction of encystation. Data are mean ± s.d. from three independent experiments (total cells counted for **b-d**, Quantification of CWP1 positive cells 4 h post induction of encystation in the indicated cell lines. **b**, dCas9-Ctrl n=626, E2F1-gRNA803 n=655; **c**, dCas9-Ctrl n=638, PAX1-gRNA438 n=640; **d**, CasRX-Ctrl n=625, ARID2-gRNA235 n=447 cells) Student's t-test, *p<0.01, **p<0.001, ****p<0.00001, ns= not significant.

**Extended Data Figure 6| Knockdown of GARP4 and MYB1 do not alter cyst viability. a**, GARP4-gRNA362 derived cysts stained with FDA (fluorescein diacetate, green) and PI (propidium iodine, magenta) to determine viability. **b,** Quantification of **a**. **c**, MYB1-gRNA1368 derived cysts stained with FDA and PI. **d,** Quantification of **c**. **e**, MYB2-gRNA669 derived cysts stained with FDA and PI. All cell lines were encysted for 48 h. Data are mean ± s.d. from three biological replicates (total cysts counted for dCas9-Ctrl n=400, GARP4-gRNA362 n=499, MYB1-gRNA1368 n=399) Student's t-test, *p<0.01, **p<0.001, ***p<0.0001, ****p<0.00001, ns= not significant. Bars, 100 µm.

**Extended Data Figure 7| Knockdowns of E2F1, PAX1, and ARID2 in *Giardia*. a-c**, Quantification of CRISPRi (or CasRX)-mediated knockdowns of E2F1 (GL50803_23756), PAX1 (GL50803_32686), and ARID2 (GL50803_8102). The expression level is normalized to the corresponding dCas9 or CasRX control. **d-f**, Immunoblots of CWP1 and tubulin from E2F1, PAX1, and ARID2 knockdowns at 4 h of encystation. **g-i**, Quantification of immunoblots of CWP1 and tubulin from E2F1, PAX1, and ARID2 knockdowns. The expression level is normalized by tubulin

control. All experiments are from three independent biological replicates. Data are mean ± s.d. (n=3) Student's t-test, *p<0.01, **p<0.001, ***p<0.0001, ****p<0.00001, ns= not significant.

**Extended Data Figure 8| Knockdown of GARP4 does not alter growth rate or cell viability. a**, Cell growth assay for dCas9 control and GARP4 knockdown strains. All cultures were started with 200,000 cells and then cell concentration was determined with a MOXI Z counter at 1, 2, and 3 days. **b**, Cell viability of dCas9 control and GARP4 knockdowns at 1, 2, 3 days as determined by ATP dependent luminescence. Three independent replicates of 200,000 cells/well were assayed in a plate reader. Black, dCas9 control. Red, GARP4-gRNA362. Green, GARP4-gRNA247. **c**, Representative images of CWP1 stained vesicles in dCas9 control and GARP4-gRNA362 cell lines. **d**, Relative CWP1 levels in GARP4 knockdowns at 4 h of encystation with lipoprotein-deficient or two step encystation media. **e**, Fluorescence level of *p*TET::GARP4-mNG with and without tetracycline induction. **f**, Relative CWP1 levels in GARP4-overexpression cell line at 4 h encystation. 20 mg/ml tetracycline were added to induce. Data are mean ± s.d. (n=3) Student's t-test, *p<0.01, **p<0.001, ****p<0.00001.

**Extended Data Figure 9| Knockdown of GARP4 increases encystation rates. a**, Quantification of CWP1 positives cells in control and GARP4 knockdown strains at 0 h, 2h, and 4h post induction of encystation. Data are mean ± s.d. from three biological replicates (total cells counted for 0 h: dCas9-Ctrl n=4927, GARP4-gRNA247 n=4927, GARP4-gRNA362 n=5808; 2h: dCas9-Ctrl n=5785, GARP4-gRNA247 n=5785, GARP4-gRNA362 n=6041, 4 h: dCas9-Ctrl n=5312, GARP4-gRNA247 n=5312, GARP4-gRNA362 n=4988 cells) Student's t-test, *p<0.01, **p<0.001, ***p<0.0001, ****p<0.00001. Bars, 100 µm.

**Extended Data Figure 10| G2/M cells have higher levels of CWP1 and MYB2. a**, CWP1-mNG fluorescence intensity of DRAQ5-stained cells at 0 and 1.5 h of encystation. **b**, MYB2-mNG fluorescence intensity of DRAQ5-stained cells at 0 and 1.5 h of encystation. **c**, Relative E2F1 levels in GARP4 knockdown cell line at 4 h of encystation. **d**, Relative PAX1 levels in GARP4 knockdown cell line at 4 h of encystation. e, GiSir2.1-mNeonGreen localization at 0 and 1.5 h post induction of encystation. Bars, 10 µm.

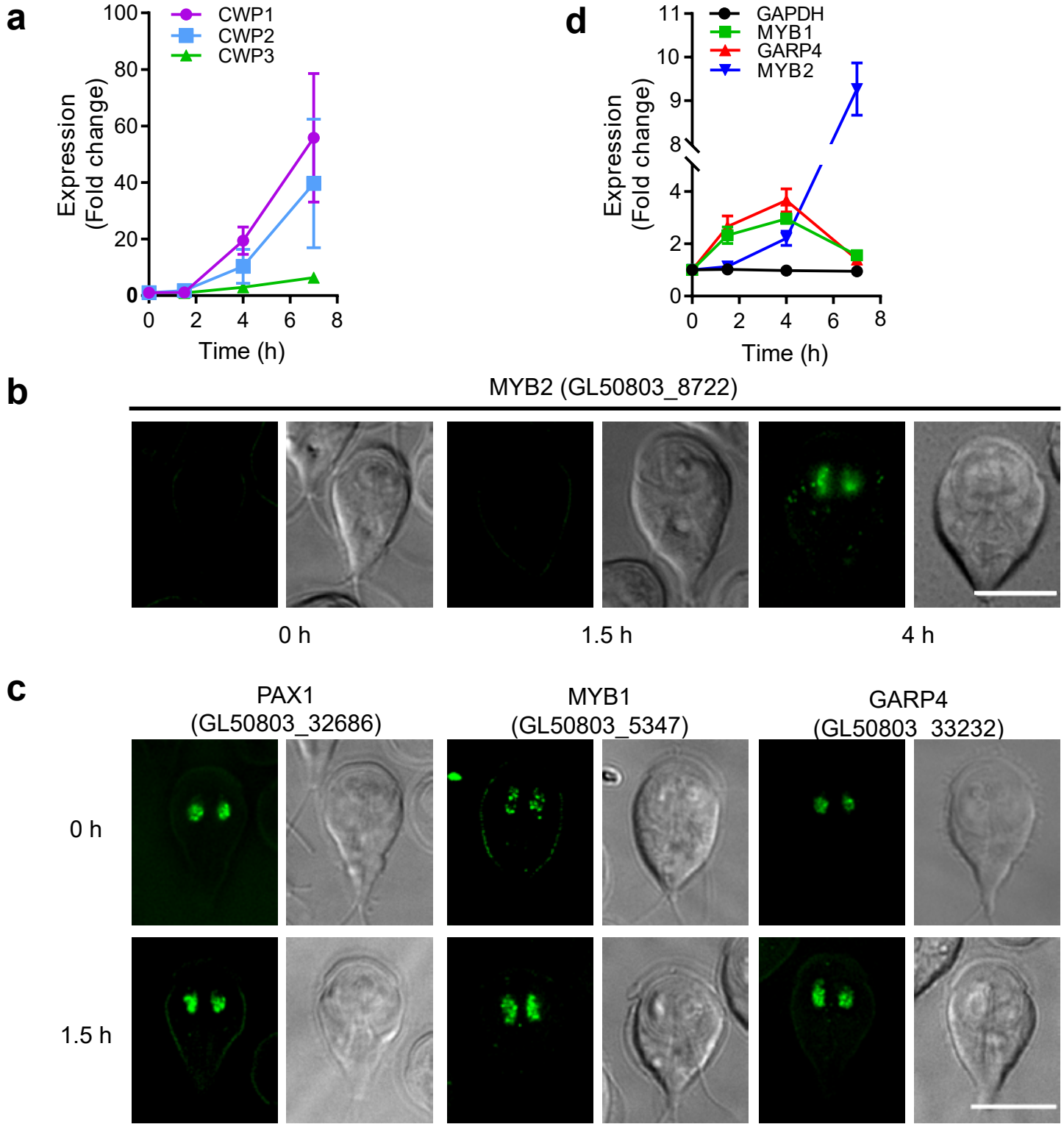


Figure 1 | GARP4 and MYB1 are early signaling TFs. a, Quantification of endogenously tagged CWP1-NLuc, CWP2-NLuc, and CWP3-NLuc after 0, 1.5, and 4 h exposure to encystation medium (Uppsala medium). Expression level from each time point has three biological replicates. Fold change is normalized to 0 h. b, Localizations of MYB2-mNG after 0, 1.5, and 4 h exposure to Uppsala medium. c, Localizations of PAX1-mNG, GARP4-mNG and MYB1-mNG after 0 and 1.5 h exposure to Uppsala medium. d, Relative expression of GARP4-NLuc, MYB1-NLuc, MYB2-NLuc, and GAPDH-NLuc after 0, 1.5, 4, 7h exposure to Uppsala medium. Expression level from each time point has three biological replicates. The fold change is normalized to 0 h. Bars, 10 μm.

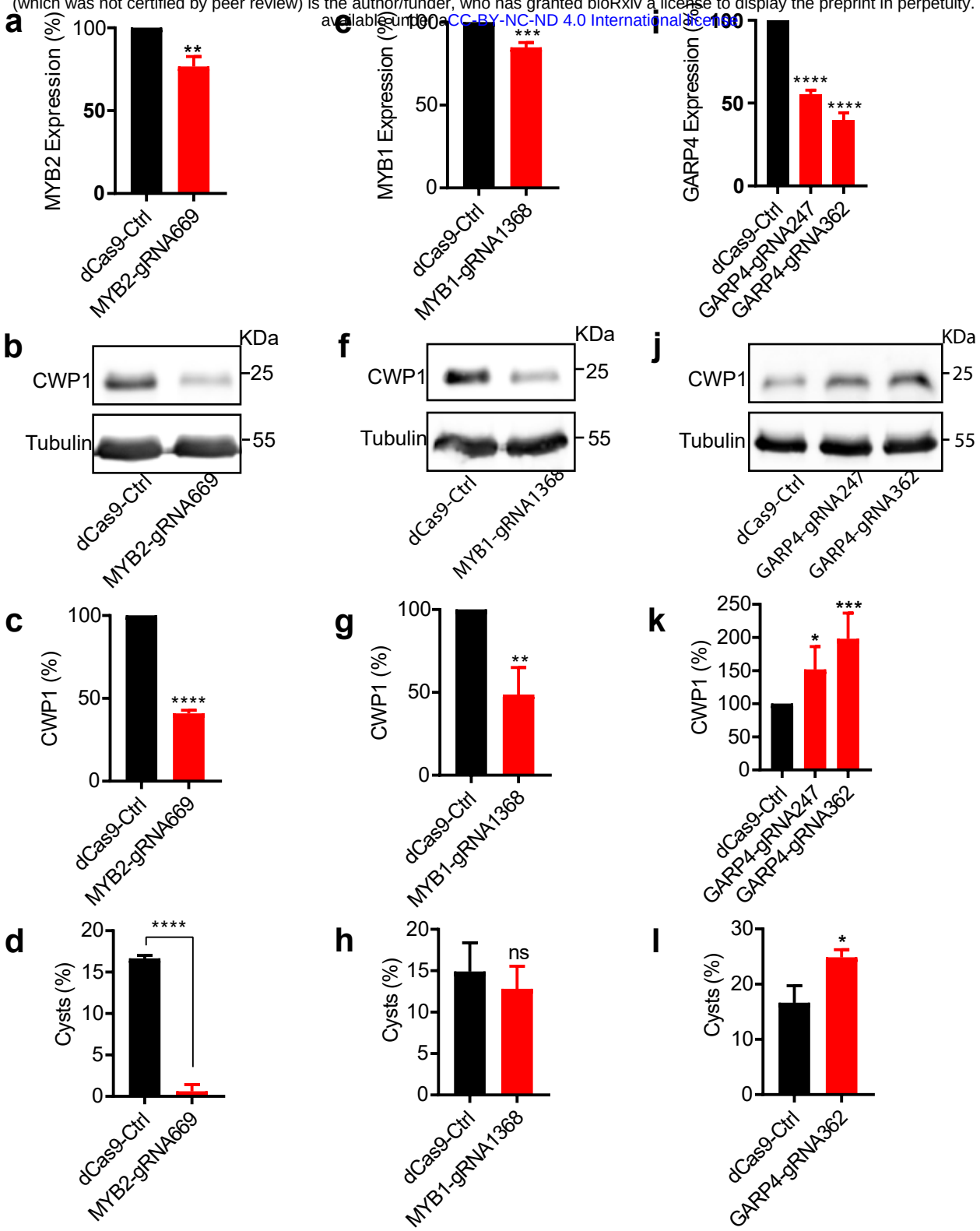


Figure 2 | Depletion of GARP4 increases CWP1 level and cyst number. a, Quantification of CRISPRi-mediated knockdowns of MYB2 at 4h into encystation. The expression level is normalized by a dCas9 control. b, Immunoblot of CWP1 and tubulin from MYB2 knockdowns at 4h into encystation. c, Quantification of immunoblots of CWP1 and tubulin from MYB2 knockdowns. The expression level is normalized to tubulin. d, Quantification of cysts for MYB2 knockdown and control after 48 h of encystation. Cyst counts were performed by hemocytometer. e, Quantification of CRISPRi-mediated knockdown of MYB1 at 1.5h into encystation. f, Immunoblot of CWP1 and tubulin from MYB1 knockdown at 4h into encystation. g, Quantification of immunoblots of CWP1 and tubulin from MYB1 knockdowns at 4h into encystation. h, Quantification of cysts for MYB1 knockdown and control after 48 h of encystation. i, Quantification of CRISPRi-mediated knockdown of GARP4 at 1.5h into encystation. j, Immunoblot of CWP1 and tubulin from GARP4 knockdown at 4h into encystation. k, Quantification of immunoblots of CWP1 and tubulin from GARP4 knockdown. l, Quantification of cyst number of GARP4 knockdown after 48 h encystation. All quantification is from three independent biological replicates which included four technical replicates for cyst counts. Data are mean ± s.d. Student's t-test, *p<0.01, **p<0.001, ***p<0.0001, ****p<0.00001, ns= not significant.

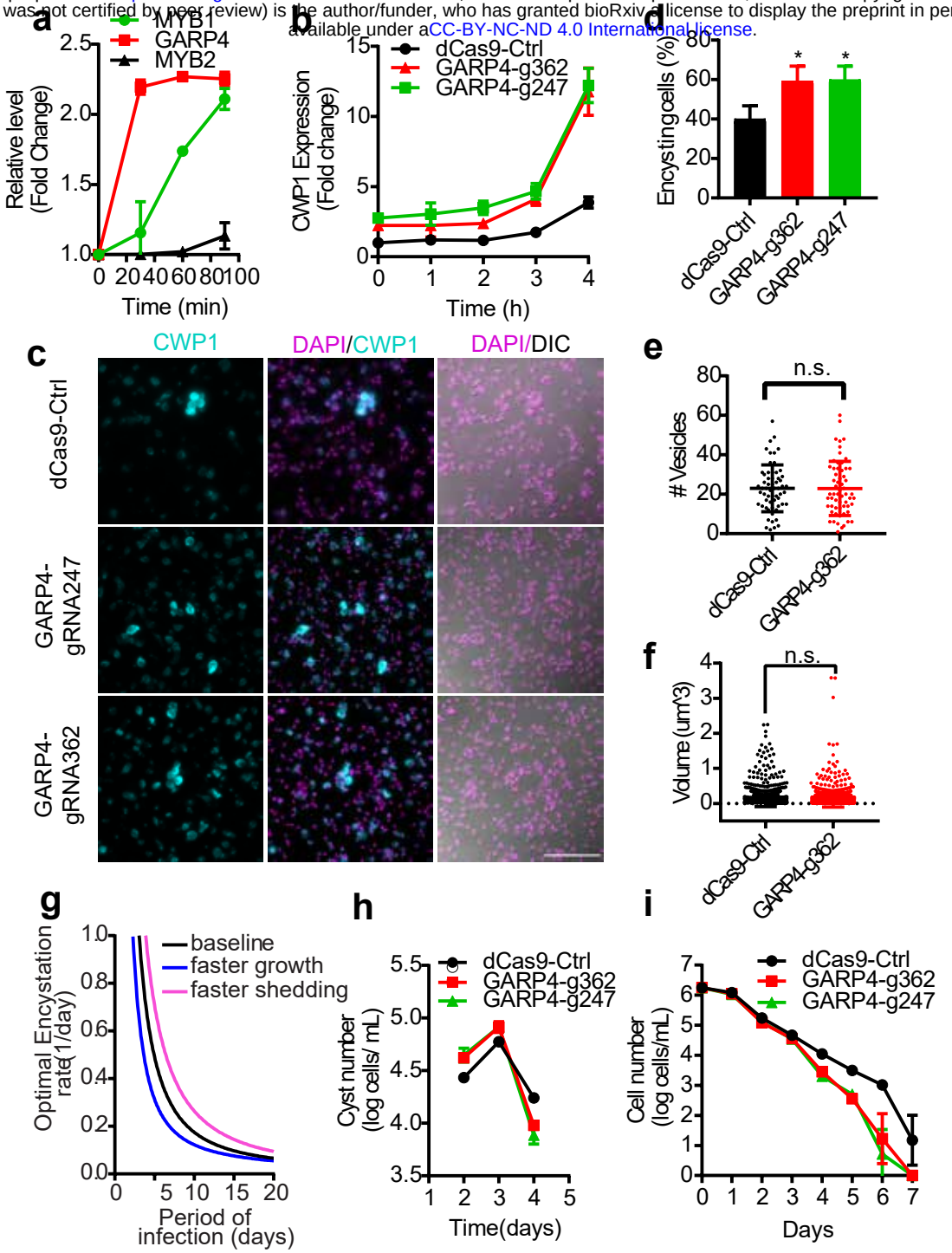


Figure 3| GARP4 regulates encystation rates. a, Relative protein levels of MYB1-NLuc, MYB2-NLuc, and GARP4-NLuc after 0, 0.5, 1 and 2 h exposure to encystation medium (Uppsala medium). The expression level from each time point has three biological replicates. The fold change is normalized to 0 h. b, Relative expression of CWP1-NLuc in GARP4 knockdowns after 0, 0.5, 1,2,3 and 4 h exposure to encystation medium (Uppsala medium). The expression level from each time point has three biological replicates. The fold change is normalized to 0 h dCas9-Ctrl. c, CWP1 and DAPI staining at 24 h of encystation for dCas9-Ctrl, GARP4-gRNA247 and GARP4-gRNA362 cell lines. Bars, 100 µm. d, Quantification of encysting cells at 24 h post induction of encystation for dCas9-Ctrl, GARP4-gRNA247 and GARP4-gRNA362 cell lines as determined by CWP1 expression. Data are mean ± s.d. from three independent experiments (total cells counted for dCas9-Ctrl n=1830, GARP4-g362 n=1747, GARP4-g247 n=1783) Student's t-test, *p<0.01. e, IMARIS-assisted analysis of vesicle number in 4 h encysting cells of dCas9-Ctrl, GARP4-gRNA247 and GARP4-gRNA362 cell lines. f, IMARIS-assisted analysis of vesicle volume of 4 h encysting cells of dCas9-Ctrl, GARP4-gRNA247 and GARP4-gRNA362 cell lines. n.s.= not significant. n=63 cells for dCas9-Ctrl. n= 93 for GARP4-g362. g, Using our dynamical model, we numerically determine the optimal encystation rate as a function of the period of infection for a baseline set of parameters (specifically, $\gamma = 0.363$ day-1, $\lambda = 0.1$ day-1, $T_0 = 1$ cell, and $C_0 = 0$ cells; see Methods). The result is the thick black curve. We then repeat the analysis but increase the rate of trophozoite growth ($\gamma = 0.762$ day-1) or increase the rate of shedding ($\lambda = 0.25$ day-1), which yields the blue and red curves, respectively. h, Quantification of cyst number in GARP4 knockdown from daily supplement of fresh encystation medium (removed detached cells and cysts). i, Quantification of trophozoite number in GARP4 knockdown from daily supplement of fresh encystation medium.

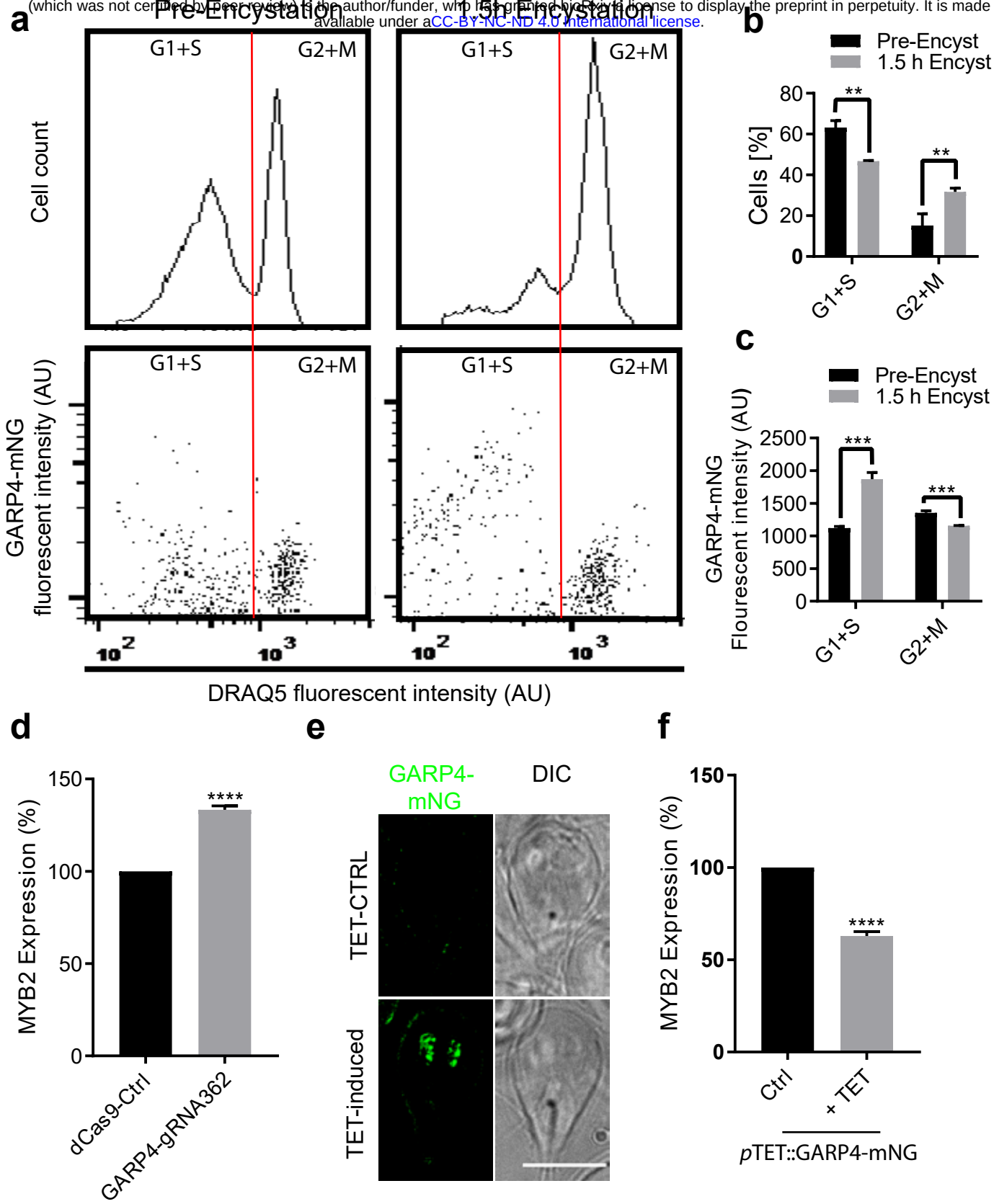


Figure 4| GARP4 is part of the restriction point that prevents G1 cells from encysting. a, Flow cytometry analysis of DRAQ5 and GARP4-mNG at 0 and 1.5 h of encystation. Red line is the separation point between G1/S and G2/M phases. b, Quantification of G1/S and G2/M cells from 0 and 1.5 h encystation. Data are mean ± s.d. (n=3, 10,000 cells per replicate) Student's t-test, **p<0.001. c, Quantification of GARP4-mNG fluorescence intensity for G1/S and G2/M cells at 0 and 1.5 h of encystation. Data are mean ± s.d. (n=3) Student's t-test, ****p<0.0001. d, Quantification of relative expressions of MYB2 from dCas9 control and GARP4-gRNA362 cell lines. ****p<0.00001. e, Fluorescent imaging of pTET::GARP4-mNG with and without tetracycline induction. Bars, 10 µm. f, Quantification of relative expressions of MYB2 after 4 h of encystation from tetracycline-induced GARP4-mNG overexpression cell lines. ****p<0.00001.